EXPLORING BUILDING HEIGHT ESTIMATION METHODS AND THEIR APPLICATIONS IN MICRO-SCALE POPULATION DATA ANALYSIS

Kittisak Maneepong[1] and Yuki Akiyama[2]
[1]Graduate Student, Graduate School of Integrative Science and Engineering, Tokyo City University
1-28-1 Tamatsuzumi, Setagaya-ku, Tokyo 158-8557
Email: g2291605@tcu.ac.jp

[2]Associate Professor, Department of Urban and Civil Engineering, Faculty of Architecture and Urban Design, Tokyo City University,
1-28-1 Tamatsuzumi, Setagaya-ku, Tokyo 158-8557
Email: akiyamay@tcu.ac.jp

KEYWORDS: Building Height Estimation, Open Data Sources, Micro-Population Data, Digital Surface Model (DSM), Morphological Operations

ABSTRACT: This paper investigates the optimal method for estimating building heights from open data sources that can be used to create micro-population data. Micro-population data can be used in various fields, including urban planning and policymaking, and has therefore attracted the attention of researchers. However, the difficulty in accessing micro-population data has been a significant obstacle for them not only in developing countries but also in developed countries, necessitating the development of micro-scale population data. The method presented in this paper aims at global applicability, which is beneficial by proposing the development of building data with a minimal budget. One of the essential data to create micro-population data is the building data, including its height, which is not commonly available as the open data. Our method is based on morphological operations on the digital surface model (DSM), which includes the local maximum/minimum filtration, and the maximum slope filtration. The study area covered in this paper is some parts of Bangkok and Tokyo, and the results are compared with the ground truth data. The results show that the method estimated building heights using local maximum/minimum filtration, and the maximum slope filtration over Bangkok obtained a 5-meter accuracy of 81.0 and 82.3 percent, respectively. The result over Shinjuku Tokyo is obtained with a 5-meter accuracy of 50.8 and 55.0 percent, respectively, while the accuracy in Hachioji is more pronounced at 65.8% and 51.9%. This suggests the acceptable use for the application with a higher margin of error, for instance, the number of floors, which can be used to create micro-scale population data. However, a higher degree of accuracy is preferable, and the factors affecting the accuracy should be considered. Further research is required to justify the quality between the open data and the higher resolution data to identify the compromise between the quality of the data and the cost.

1. INTRODUCTION

Understanding population is crucial for effective urban planning and resource allocation, particularly in areas such as transportation planning, disaster mitigation, and epidemic management (Hay et al., 2005; Hossain and Meng, 2020; Li et al., 2022; Mohanty and Simonovic, 2021; Nishimoto et al., 2016, p. 20; Rogers et al., 2014; Smith et al., 2019; Weiss et al., 2020, p. 20). Population data is primarily obtained through population censuses, generally conducted every 5 to 10 years, which are widely used and publicly accessible (United Nations, Department of Economic and Social Affairs, Population Division, 2019). However, collecting and analyzing population data is a resource-intensive and time-consuming task. Additionally, traditional population censuses often lack spatially detailed information on population distribution and are usually conducted at a macro level. Furthermore, they face challenges in capturing temporal changes due to the fluctuating boundaries of administrative units that govern data collection processes.

In addition to conventional censuses, alternative techniques to obtain micro-level population data through geospatial data were proposed (Chen et al., 2021; Pajares et al., 2021; Yao et al., 2017), providing a more detailed understanding of population distribution, enabling their application in various domains. Using geodata, such as building floor areas and their footprints, is common in estimating micro-population data. (Akiyama et al., 2019, 2013; Pajares et al., 2021). Studies have suggested using various building data, such as floor count, building usage, and building footprints, to estimate building-scale population. However, during our replication efforts, we encountered limited availability of such data, particularly in developing countries, where most data is either unavailable or restricted by commercialization. Additionally, the accuracy of population estimation using open data sources has not been explored in detail, particularly in developing regions and smaller cities.

As part of our core objective, our study aims to address the issue of population distribution. Specifically, we have conducted a brief research investigation on the estimation of population at the building level. Previous studies have primarily focused on estimating population at the grid level by combining multiple geospatial data sources. Table 1 provides an examination and classification of the auxiliary data commonly employed in contemporary population mapping studies. Notably, land cover data have been extensively utilized in previous research endeavors (Zandbergen and Ignizio, 2010). Researchers have demonstrated interest in socio-economic factors, including property ownership, as well as building information encompassing type and height. Such building information allows for higher-resolution settlement delineation and a detailed understanding of built-up spaces (Calka et al., 2017; Chen et al., 2021; Pajares et al., 2021; Schug et al., 2021; Wang et al., 2021; Yao et al., 2017). Night lights data have also been integrated into population estimation in several studies (Chen et al., 2021; Lloyd et al., 2017; Sorichetta et al., 2015; Zandbergen and Ignizio, 2010). However, the correlation between night lights and population estimation has been subject to debate, as utilizing night lights data has shown a tendency to overestimate population in areas with high light intensity and underestimate population in regions with lower light intensity (Sorichetta et al., 2015; Zandbergen and Ignizio, 2010). However, limited research has been conducted specifically on estimating population at the building level.

Despite the availability of sub-meter satellite imagery, the cost of accessing such data remains significantly high, and limited access (Dare, 2005). Therefore, we have chosen to utilize openly available building data, including building footprints and building height information, for our population estimation. Recent studies have explored the estimation of building height using open data sources (Huang et al., 2022; Milojevic-Dupont et al., 2020; Yang and Zhao, 2022). Various techniques have been employed to identify ground features, such as maximum slope filtration (Vosselman, 2000) or identification of local minima (Huang et al., 2022). However, it is important to note that these experiments were conducted using higher resolution input data, as methodologies successful at higher resolutions may not yield accurate results at lower resolutions.

Table 1:State-of-the-art about auxiliary data in population mapping

Auxiliary data Review		*2010-2016*	*2017-2022*
Built-up	Building Footprints		(Calka et al., 2017; Chen et al., 2021; Pajares et al., 2021; Schug et al., 2021; Wang et al., 2021)
	Building Height		(Balakrishnan, 2020; Calka et al., 2017; Chen et al., 2021; Schug et al., 2021)
	Building Type		(Calka et al., 2017; Chen et al., 2021; Pajares et al., 2021; Schug et al., 2021; Shang et al., 2021; Wang et al., 2021; Yao et al., 2017)
	Road Cover	(Sorichetta et al., 2015; Worldpop, 2013; Zandbergen and Ignizio, 2010)	(Balakrishnan, 2020; Lloyd et al., 2017)
Surface	Land Cover	(Azar et al., 2013; Sorichetta et al., 2015; Worldpop, 2013; Zandbergen and Ignizio, 2010)	(Balakrishnan, 2020; European Commission. Joint Research Centre., 2019; Facebook Connectivity Lab and Center for International Earth Science Information Network - CIESIN - Columbia University, 2016; Pajares et al., 2021; Sorichetta et al., 2015)
	Land Use		(Balakrishnan, 2020)
	Terrain Elevation	(Azar et al., 2013)	
Environment	Night Lights	(Sorichetta et al., 2015; Worldpop, 2013; Zandbergen and Ignizio, 2010; Zeng et al., 2011)	(Chen et al., 2021; Li and Zhou, 2018; Lloyd et al., 2017)
	Climate	(Sorichetta et al., 2015; Worldpop, 2013)	(Lloyd et al., 2017)

In this context, we assume that all buildings have a consistent shape from the base to the top throughout their height. This assumption allows us to simplify the estimation process by considering a uniform structure for all buildings included in our analysis. While this assumption may not capture the diverse architectural characteristics of real-world buildings, it provides an approximation that aids in the estimation of population at the building level.

We aim to bridge the gap by proposing a methodology for estimating the population at the building scale using open data sources. Our objective is to develop a global and cost-effective approach that accurately estimates the population at the building level. The proposed methodology involves the fusion of building information with population data, leveraging state-of-the-art techniques. This fusion approach enhances the accuracy and granularity of population estimation by considering individual building characteristics. This study focuses explicitly on estimating building height

using open data sources, a critical component of building data. We conducted tests by reproducing previous techniques and comparing each approach using case studies in Bangkok and Tokyo, comparing the results with ground truth data.

2. DATASETS AND STUDY AREA

The data utilized for this study were carefully chosen based on the criterion of being open, accessible, and current. The following section presents the precise data that has been selected.

2.1 ALOS World 3D

In the quest to estimate building heights, we sought the most recent and openly accessible Digital Surface Model (DSM). Advanced Land Observing Satellite (ALOS) World 3D (AW3D30) dataset (Earth Observation Research Center, Japan Aerospace Exploration Agency (JAXA EORC), 2016) considered is chosen considering both openness and resolution. The AW3D30 dataset provides high-resolution terrain data with a horizontal resolution of 30 meters and a vertical accuracy of 5 meters. Encompassing global land areas, the AW3D30 dataset was created using data gathered by the PRISM (Panchromatic Remote-Sensing Instrument for Stereo Mapping) onboard the ALOS satellite, which was active from 2006 to 2011.

2.2 GlobalMLBuildingFootprints

We utilized the shape of buildings data from the GlobalMLBuildingFootprints dataset provided by Microsoft. This dataset, created using Bing Map imagery spanning from 2014 to 2023, supports the generation of building edges through two techniques: semantic segmentation, which involves the classification of each pixel in the image into a category, and polygonization, a process that converts pixelated shapes into polygonal forms. These techniques have been thoroughly validated and deliver an impressive accuracy rate exceeding 90% (Microsoft, 2023)

2.3 NASADEM

In conjunction with DSM data, the digital elevation model (DEM) derived from the Shuttle Radar Topography Mission (SRTM) provides the ground references at 30 meters resolution (NASA JPL, 2020). This data serves as a reference. Data from AW3D30 will guide the primary estimation.

2.4 Study Area

The study area encompassed four distinct socio-economic regions, two areas in Tokyo, and combined two areas of Bangkok, Thailand, considering variables such as relative population density land use. Table 2 shows the deviation in terrain using NASADEM as a reference.

Table 2:Elevation Information of Selected Urban Areas in Tokyo and Bangkok

Area	Average Elevation (m)	SD of Elevation (m)
Shinjuku, Tokyo	35.48	10.86
Hachioji, Tokyo	215.57	134.55
Saphan Sung, Bangkok	2.30	2.49
Vadhana, Bangkok	3.64	7.04

2.4.1 Tokyo

Shinjuku, Tokyo, renowned as an administrative, transportation, and commercial hub, stands out as one of the most densely populated areas. The population within an 18-square-kilometer area (Geospatial Information Authority of Japan(GSI), 2016) reaches 346,000 (Statistics Division, Bureau of General Affairs, 2022), approximately 19,000 individuals per square kilometer. The landscape is dominated by towering buildings and expansive shopping malls.

Hachioji City, located in the western part of the Tokyo metropolitan area, is known for its picturesque natural surroundings and outdoor recreational opportunities. The area features mountainous terrain and easy access to numerous hiking trails and parks. Despite its suburban location, Hachioji City exhibits a comparatively low population density compared to other parts of Tokyo, housing approximately 561,000 people within an area of 186.38 square kilometers (Geospatial Information Authority of Japan(GSI), 2016; Statistics Division, Bureau of General Affairs, 2022). This translates to an approximate population density of 4,900 individuals per square kilometer.

2.4.2 Bangkok

Situated in the northeastern region of Bangkok, Saphan Sung District is characterized by its suburban geographical features and covers an area of approximately 28.1 square kilometers. The district's strategic location, in close proximity to the airport train network, has had a significant impact on the area's development trajectory. Saphan Sung has played a key role in fostering the growth of the surrounding region and is widely recognized as a suburb characterized by a harmonious blend of residential and commercial development.

Wattana, another district in Bangkok, covers an area of 12.56 square kilometers and is home to approximately 80,800 (Open Government Data of Thailand, 2021). Wattana is geographically located in the heart of Bangkok. It is known for its affluence and cosmopolitan ambiance. The district boasts a developed landscape with an array of high-rise, low-rise, and commercial buildings, complemented by excellent connectivity to other areas through an extensive train network. Wattana is a dynamic and diverse neighborhood that is home to both Thai and foreign residents. The area offers a wide range of amenities, including upscale boutiques, restaurants, and entertainment venues. It is widely recognized as one of Bangkok's most affluent and desirable neighborhoods, characterized by high property values and an elevated standard of living.

For our study, we will analyze both Bangkok districts, consolidating them into one model. This merger is aimed at enlarging the sample size and enhancing our ability to obtain accurate ground truth data for research purposes.

3. METHOD TESTED

Our study assesses two methodologies that use the ALOS World 3D DSM to estimate building height. The most widespread of these techniques entails extracting ground elevation data directly from the DSM. At the current stage of our research, the building shape is primarily employed as a reference and means of storing the respective building heights. Rather than focusing on intricate architectural details, our analysis emphasizes the utilization of building shape as a basic framework for height representation. This simplified approach allows us to effectively integrate the height information within our population estimation methodology, while minimizing the complexity associated with considering the unique geometric characteristics of individual buildings.

3.1 Sliding Windows

The sliding window technique is employed to "normalize" the DSM by utilizing the minimum and maximum values within a window (Huang et al., 2022). The slope correction is facilitated by integrating NASADEM, which aids in determining the slope. This method involves applying a filter that replaces each pixel value with the minimum or maximum value within its neighboring vicinity. The slope correction is primarily based on terrain data obtained from NASADEM, particularly in regions where the slope exceeds 10 degrees.

The data used for our analysis is the DSM, which can be visualized as a matrix of pixels. Mathematically, the DSM matrix is denoted as:

$$DSM = \begin{bmatrix} x_{00} & \cdots & x_{0n} \\ \vdots & \ddots & \vdots \\ x_{m0} & \cdots & x_{mn} \end{bmatrix} \quad (1)$$

Where eachx_{ij} represents the pixel value at position (i, j) in the DSM matrix. The neighboring values of x_{ij} can be identified as:

$$DSM_{ij} = \begin{bmatrix} x_{(i-1)(j-1)} & x_{(i-1)j} & x_{(i-1)(j+1)} \\ x_{i(j-1)} & x_{ij} & x_{i(j+1)} \\ x_{(i+1)(j-1)} & x_{(i+1)j} & x_{(i+1)(j+1)} \end{bmatrix} \quad (2)$$

In order to find the minimum and maximum points, two matrices are created. The $max(DSM)$ matrix stores the maximum value within the 3-by-3 neighborhood for each pixel, while the $min(DSM)$ matrix stores the minimum value. These matrices have the same dimensions as the DSM.

$$max(DSM) = \begin{bmatrix} max(DSM_{(0,0)}) & \cdots & max(DSM_{(0,n)}) \\ \vdots & \ddots & \vdots \\ max(DSM_{(m,0)}) & \cdots & max(DSM_{(m,n)}) \end{bmatrix} \quad (3)$$

$$min(DSM) = \begin{bmatrix} \min(DSM_{(0,0)}) & \dots & \min(DSM_{(0,n)}) \\ \vdots & \ddots & \vdots \\ \min(DSM_{(m,0)}) & \dots & \min(DSM_{(m,n)}) \end{bmatrix} \quad (4)$$

Then, normalize the DSM, the difference between the local maximum and minimum values is calculated. This is done by subtracting the $min(DSM)$ matrix from the $max(DSM)$ matrix. The result represents the normalized DSM, denoted as $nDSM$.

$$\mathrm{nDSM} = \max(\mathrm{DSM}) - \min(\mathrm{DSM}) \quad (5)$$

Slope correction is applied to the normalized DSM to account for the slope of the terrain. The minimum DSM matrix is used to calculate the slope correction, denoted as $slope_{cor}$, terrain data from NASADEM is employed as a reference for slope values. Steps 1-3 are repeated using the $min(DSM)$ as the input.

The final step involves calculating the corrected normalized DSM, denoted as $cDSM_{ij}$, based on slope conditions. The terrain model from NASADEM is used as a reference for the slope. If the slope value at position (i,j), denoted as $slope_{ij}$, is greater than or equal to a threshold percentage (x%), the corrected DSM value is obtained by subtracting the slope correction from the normalized DSM value. If the slope value is less than the threshold percentage, the corrected DSM value remains the same as the normalized DSM value.

$$cDSM_{ij} = \begin{cases} \mathrm{n}DSM_{ij} - \mathrm{slope}_{\mathrm{cor}_{ij}}, & \text{if } \mathrm{slope}_{ij} \geq x\% \\ \mathrm{n}DSM_{ij}, & \text{if } \mathrm{slope}_{ij} < x\% \end{cases} \quad (6)$$

Where: $cDSM_{ij}$ = the corrected DSM at position (i,j),

$nDSM_{ij}$ = the normalized DSM at position (i,j),

$slope_{ij}$ = the slope value at position (i,j),

$Slope_{cor_{ij}}$ = the slope correction based on terrain data, and

$x\%$ = the threshold slope percentage.

In summary, this calculation method aims to identify local minimum and maximum values in a DSM and then normalize the DSM by accounting for slope conditions. The resulting corrected DSM can provide enhanced information about the analyzed terrain or surface.

3.2 Slope-based

Utilize the terrain filtration technique to the DSM data, to filter the terrain (Vosselman, 2000).

$$DEM = \mathrm{p_i} \in A | \forall \mathrm{p_j} \in A : \mathrm{h_{p_i}} - \mathrm{h_{p_j}} \leq \Delta \mathrm{h_{max}} \left(\mathrm{d}(\mathrm{p_i}, \mathrm{p_j}) \right) \quad (7)$$

Let A represent the set of all points, and DEM denote the set of ground points. A point $\mathrm{p_i}$ is classified as a terrain point if there does not exist another point $\mathrm{p_j}$ such that the height difference between $\mathrm{p_i}$ and $\mathrm{p_j}$ exceeds the maximum allowed height difference at the distance between these points.

Subsequent to the exclusion of areas exceeding the maximum slope, the ground elevation is interpolated using the Inverse distance weighted (IDW) to replenish the terrain (Shepard, 1968).

$$Z(x) = \frac{\sum w_i Z_i}{\sum w_i}; w_i = 1/d_i^p \quad (8)$$

For estimating the value at a particular location within a spatial domain, a weighted average of observed values near that location is employed. This approach assigns weights that are inversely proportional to the distances between the points, thus assigning greater weights to points in closer proximity. The weight w_i is defined as $w_i = \frac{1}{d_i^p}$, where d_i represents the distance between the point of interest x and the data point Z_i. The parameter p is a power parameter that modulates the weight assigned to data points based on their distance from x. This approach ensures that closer data points exert a greater influence on the estimated value at x.

4. RESULT

In a comparative analysis between two methods, sliding window and slope-based, the performance metrics of height prediction were evaluated in three different areas: Shinjuku (Tokyo), Hachioji (Tokyo), and Vadhana-Saphan Sung (Bangkok). The metrics used to evaluate the performance of these methods were Mean Absolute Error (MAE), Root Mean Squared Error (RMSE), R-squared, Relative Absolute Error (RAE), Relative Squared Error (RSE), Prediction Bias, and Accuracy Percentage within thresholds of ±1m, ±2m, and ±5m.

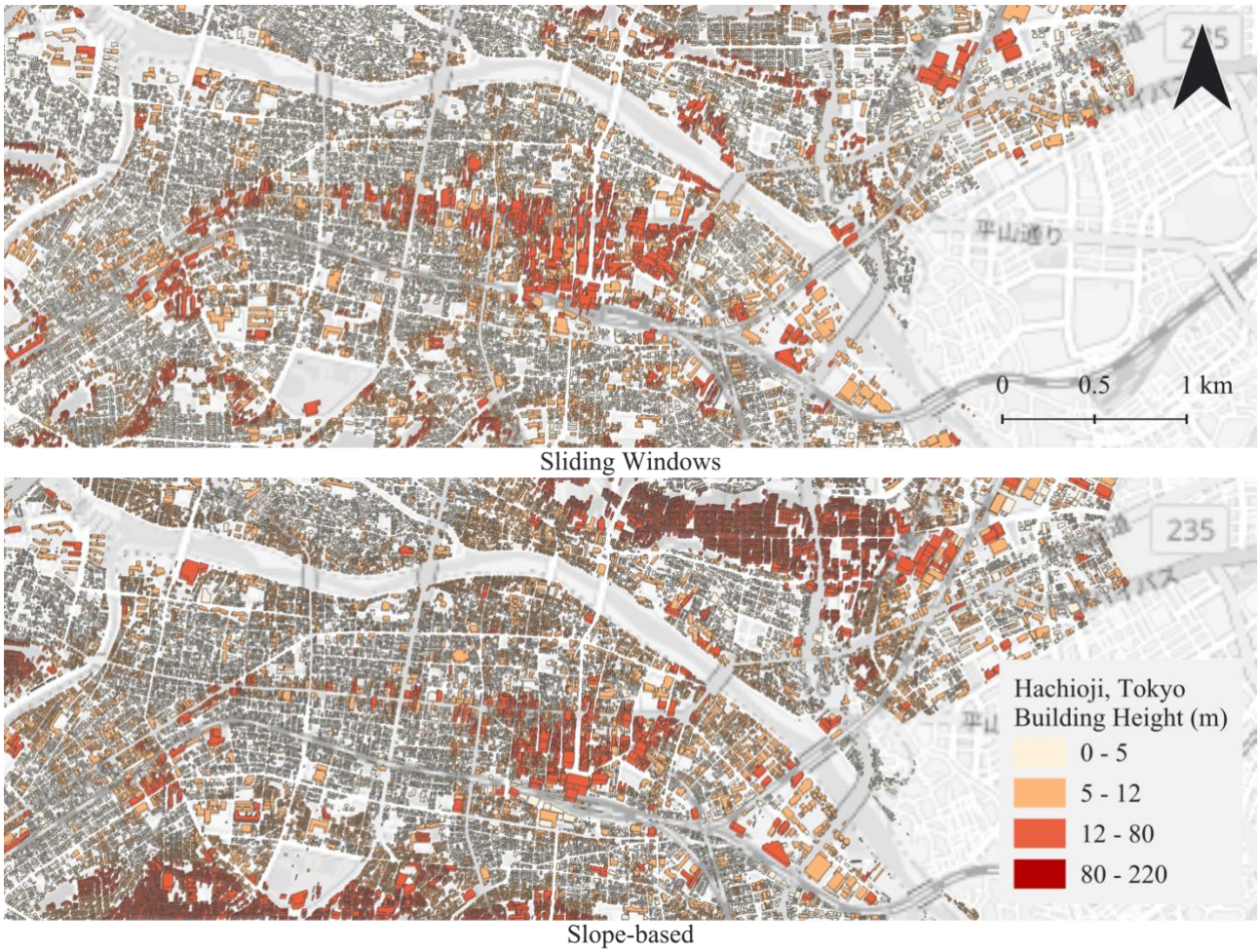

Figure 1: Result Visualization over Hachioji, Tokyo

Table 3:Comparative Results Metrics and Accuracy

	Shinjuku, Tokyo		Hachioji, Tokyo		Vadhana-Saphan Sung, Bangkok	
Metric	Sliding windows	Slope based	Sliding windows	Slope based	Sliding windows	Slope based
MAE	6.37	5.73	4.50	8.53	4.46	4.07
RMSE	9.21	8.36	5.67	13.45	8.80	8.31
R-Squared	-0.19	-0.01	-1.69	-14.83	-0.09	0.03
RAE	1.33	1.07	3.50	5.77	1.32	1.21
RSE	1.19	1.01	2.69	15.83	1.09	0.97
Prediction Bias	-5.04	-3.37	-2.56	4.08	-2.18	-3.46
% Accuracy ±1 m	10.4%	12.1%	12.6%	10.1%	15.6%	13.9%
% Accuracy ±2 m	19.6%	23.5%	24.2%	20.8%	31.4%	30.3%
% Accuracy ±5 m	50.8%	55.0%	65.8%	51.9%	81.0%	82.3%

In the Shinjuku area of Tokyo, the sliding windows method yielded an MAE of 6.37, while the slope-based method had a slightly lower MAE of 5.73. However, both methods had comparable RMSE values of 9.21 for the sliding windows method and 8.36 for the slope-based method. Interestingly, the R-squared value for the sliding windows method (-0.19) was closer to zero compared to the slope-based method (-0.01), suggesting a slightly better fit of the model to the data for the latter.

For the Hachioji area in Tokyo, the sliding windows method outperformed the slope-based method in terms of MAE, with values of 4.50 and 8.53, respectively. The RMSE for the sliding windows method was significantly lower at 5.67 compared to 13.45 for the slope-based method. This large difference indicates a much better prediction accuracy for the sliding windows method in this region. The R-squared values further emphasize this difference, with the Sliding windows method showing -1.69 and the Slope-based method showing a much lower value of -14.83.

In contrast, for the Vadhana-Saphan Sung area in Bangkok, the differences between the two methods were less pronounced. The MAE for the sliding window method was 4.46, slightly higher than the 4.07 for the slope-based method. Both methods showed similar RMSE values of 8.80 for sliding windows and 8.31 for slope-based. The R-squared values were closer to zero for both methods, indicating a better fit to the data compared to the other regions.

In terms of accuracy percentages, there were different results for the three regions. In Shinjuku, the Slope-based method showed higher accuracy at all three thresholds, with the most significant difference observed at the ±5 m threshold (55.0% for Slope-based vs. 50.8% for Sliding windows). In Hachioji, however, the sliding window method was superior in accuracy at both the ±2m and ±5m thresholds. For the Vadhana-Saphan Sung area, the Slope-based method slightly outperformed at the ±5m threshold, with an accuracy of 82.3% compared to 81.0% for the Sliding windows method.

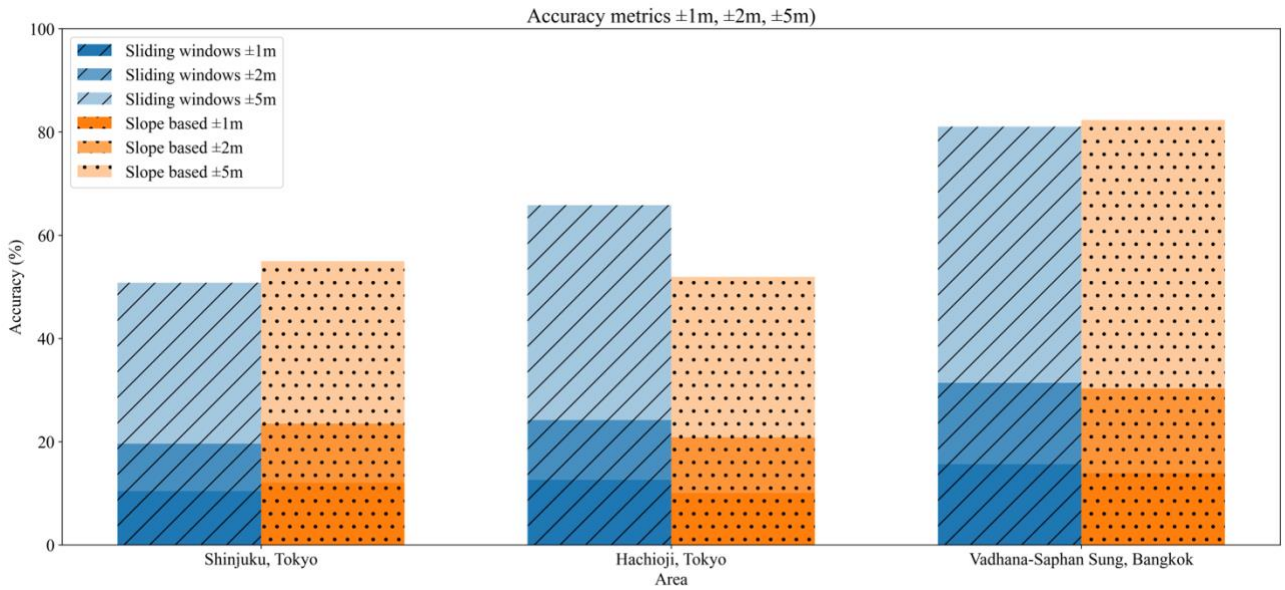

Figure 2: Comparative Accuracy of Sliding Windows and Slope-based

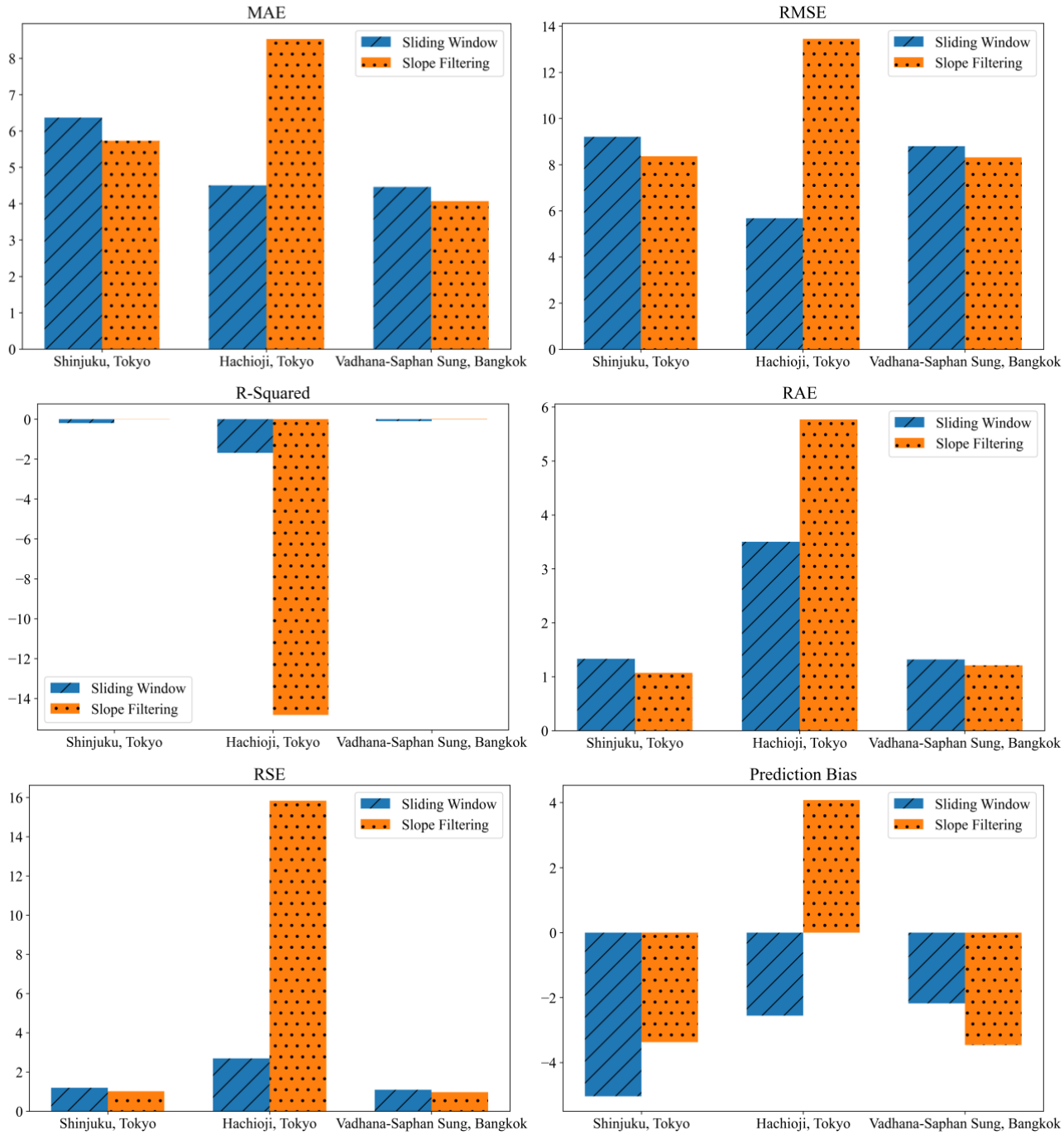

Figure 3: Comparison Plot of Each Method Evaluation Metrics

5. CONCLUSION

The results of two height prediction methodologies: the Sliding windows and Slope-based approaches, focusing on three geographically distinct regions: Shinjuku and Hachioji in Tokyo, and Vadhana-Saphan Sung in Bangkok. The results revealed nuanced variations in the performance of both methods across the selected areas.

1. In Shinjuku, Tokyo, the Slope-based method exhibited marginally superior predictive accuracy, particularly evident in the MAE and accuracy percentage metrics.

2. Conversely, in Hachioji, Tokyo, the Sliding windows method showcased better prediction accuracy, as highlighted by its lower MAE and RMSE.

3. For Vadhana-Saphan Sung, Bangkok, both methods demonstrated similar performance, with minor advantages for the Slope-based approach in specific metrics.

The disparities in the efficacy of the two methods across regions underscore the importance of regional factors in height prediction. Furthermore, neither method universally outperformed the other, indicating the need for a context-specific approach in selecting the appropriate methodology. Indicate that, overall, it can be observed that the slope-based filtering technique tends to exhibit superior performance in regions of lower complexity when compared to the sliding window technique. However, the employed techniques tend to result in underestimations and negative R-squared values. This suggests that the estimations may not strongly correlate with the ground truth values. However, the accuracy metrics demonstrate a relatively high degree of precision for flat terrains, such as those found in Bangkok with the sliding window technique.

6. DISCUSSION

Building height plays a crucial role in building data analysis as it facilitates the estimation of population at the building scale. By understanding the height of a building, we gain valuable insights into the approximate area occupied by each structure. Notably, the use of sliding windows in building height estimation has proven to be more effective in flat terrains. Research findings indicate that such methodologies can achieve up to 80% accuracy when estimating building height on a preliminary basis. This demonstrates the potential of sliding windows in accurately gauging vertical dimensions when the terrain exhibits relative flatness.

The accuracy of building height estimation is influenced by several factors, including the resolution of the input data and terrain variations. It is important to note that the resolution of the input data, at 30 meters, may be relatively coarse for detached buildings. The DSM data may not accurately represent the ground surrounding the building and the building itself. Furthermore, the relatively coarse resolution of the input DSM data may pose challenges in representing high structures surrounded by lower structures, as the elevation data is averaged within a 30m-by-30-m grid. This phenomenon has been empirically observed to lead to overestimations for structures of lower height and underestimations for structures of greater height. The higher resolution of the input data can result in a better correlation (Li et al., 2020). Additionally, terrain variations significantly impact the results.

To further enhance this study, future research could focus on obtaining higher-quality input data or exploring the application of machine learning (ML) techniques directly on satellite imagery. However, it is essential to note that accessing openly available very high-resolution satellite images may pose challenges at present. Nonetheless, investigating alternative approaches beyond stereo image, DSM, holds promise for expanding the scope of the study. Exploring advanced ML algorithms, such as convolutional neural networks (CNNs), could potentially enable the direct analysis of satellite imagery without relying on stereo pairs. By leveraging the rich spatial information captured in high-resolution satellite images, ML models can learn complex patterns and features related to building height estimation. This approach may offer increased accuracy and efficiency compared to traditional methodologies using stereo imagery. Furthermore, it can be beneficial to validate results using commercialized higher-resolution data (sub-meter) to assess their significance in quality of the result. This approach allows for real-world application.

The estimation of building height is expected to be utilized in population estimation at the building level. One potential approach in building height estimation and population disaggregation is the utilization of direct height or floor information, combined with a micro-scale dasymetric modeling approach (Akiyama et al., 2019). However, the aim of this study is to advance beyond relying solely on auxiliary data and investigate the application of machine learning techniques, once the auxiliary data becomes more comprehensive and detailed. By enriching the auxiliary dataset, we aim to achieve more refined estimations, thereby enhancing the understanding of building height dynamics and improving population disaggregation at a higher resolution level.

The result can potentially be further applied in various approaches. For example, conventional transportation planning approaches typically utilize aggregated population data within specific zones of interest; nevertheless, including micro-population data allows for a more detailed consideration of traffic flow specifics and transportation system demand. Similarly, integrating population distribution into disaster management enhances comprehension of at-risk populations and facilitates more efficient evacuation plans. Additionally, micro-population data proves valuable in epidemic management by enabling precise estimation of medical resource needs to be grounded in population distribution.

Overall, the estimation of building height offers potential insights into population dynamics and can revolutionize various domains by enabling more detailed and data-driven decision making. By considering the impact of terrain variations, leveraging higher-resolution input data, and continuously refining estimation techniques, it is possible to use all potential of building height estimation for enhanced urban planning and resource allocation.

7. REFERENCE

Akiyama, Y., Miyazaki, H., Sirikanjanaanan, S., 2019. Development of micro population data for each building: Case study in Tokyo and Bangkok, in: 2019 First International Conference on Smart Technology Urban Development (STUD). Presented at the 2019 First International Conference on Smart Technology Urban Development (STUD), pp. 1–6. https://doi.org/10.1109/STUD49732.2019.9018851

Akiyama, Y., Takada, H., Shibasaki, R., 2013. Development of Micropopulation Census through Disaggregation of National Population Census. conference papers.

Azar, D., Engstrom, R., Graesser, J., Comenetz, J., 2013. Generation of fine-scale population layers using multi-resolution satellite imagery and geospatial data. Remote Sensing of Environment 130, 219–232. https://doi.org/10.1016/j.rse.2012.11.022

Balakrishnan, K., 2020. A method for urban population density prediction at 30m resolution. Cartography and Geographic Information Science 47, 193–213. https://doi.org/10.1080/15230406.2019.1687014

Calka, B., Nowak Da Costa, J., Bielecka, E., 2017. Fine scale population density data and its application in risk assessment. Geomatics, Natural Hazards and Risk 8, 1440–1455. https://doi.org/10.1080/19475705.2017.1345792

Chen, H., Wu, B., Yu, B., Chen, Z., Wu, Q., Lian, T., Wang, C., Li, Q., Wu, J., 2021. A New Method for Building-Level Population Estimation by Integrating LiDAR, Nighttime Light, and POI Data. Journal of Remote Sensing 2021, 1–17. https://doi.org/10.34133/2021/9803796

Dare, P.M., 2005. Shadow Analysis in High-Resolution Satellite Imagery of Urban Areas. Photogrammetric Engineering & Remote Sensing 71, 169–177. https://doi.org/10.14358/PERS.71.2.169

Earth Observation Research Center, Japan Aerospace Exploration Agency (JAXA EORC), 2016. ALOS Global Digital Surface Model "ALOS World 3D - 30m (AW3D30)."

European Commission. Joint Research Centre., 2019. GHSL data package 2019: public release GHS P2019. Publications Office, LU.

Facebook Connectivity Lab and Center for International Earth Science Information Network - CIESIN - Columbia University, 2016. High Resolution Settlement Layer (HRSL).

Geospatial Information Authority of Japan(GSI), 2016. Global Map Japan.

Hay, S.I., Noor, A.M., Nelson, A., Tatem, A.J., 2005. The accuracy of human population maps for public health application. Trop Med Int Health 10, 1073–1086. https://doi.org/10.1111/j.1365-3156.2005.01487.x

Hossain, M.K., Meng, Q., 2020. A fine-scale spatial analytics of the assessment and mapping of buildings and population at different risk levels of urban flood. Land Use Policy 99, 104829. https://doi.org/10.1016/j.landusepol.2020.104829

Huang, H., Chen, P., Xu, X., Liu, Caixia, Wang, J., Liu, Chong, Clinton, N., Gong, P., 2022. Estimating building height in China from ALOS AW3D30. ISPRS Journal of Photogrammetry and Remote Sensing 185, 146–157. https://doi.org/10.1016/j.isprsjprs.2022.01.022

Li, C., Liu, M., Hu, Y., Wang, H., Zhou, R., Wu, W., Wang, Y., 2022. Spatial distribution patterns and potential exposure risks of urban floods in Chinese megacities. Journal of Hydrology 610, 127838. https://doi.org/10.1016/j.jhydrol.2022.127838

Li, X., Zhou, W., 2018. Dasymetric mapping of urban population in China based on radiance corrected DMSP-OLS nighttime light and land cover data. Science of The Total Environment 643, 1248–1256. https://doi.org/10.1016/j.scitotenv.2018.06.244

Li, X., Zhou, Y., Gong, P., Seto, K.C., Clinton, N., 2020. Developing a method to estimate building height from Sentinel-1 data. Remote Sensing of Environment 240, 111705. https://doi.org/10.1016/j.rse.2020.111705

Lloyd, C.T., Sorichetta, A., Tatem, A.J., 2017. High resolution global gridded data for use in population studies. Sci Data 4, 170001. https://doi.org/10.1038/sdata.2017.1

Microsoft, 2023. GlobalMLBuildingFootprints.

Milojevic-Dupont, N., Hans, N., Kaack, L.H., Zumwald, M., Andrieux, F., De Barros Soares, D., Lohrey, S., Pichler, P.-P., Creutzig, F., 2020. Learning from urban form to predict building heights. PLoS ONE 15, e0242010. https://doi.org/10.1371/journal.pone.0242010

Mohanty, M.P., Simonovic, S.P., 2021. Understanding dynamics of population flood exposure in Canada with multiple high-resolution population datasets. Science of The Total Environment 759, 143559. https://doi.org/10.1016/j.scitotenv.2020.143559

NASA JPL, 2020. NASADEM Merged DEM Global 1 arc second V001. https://doi.org/10.5067/MEASURES/NASADEM/NASADEM_HGT.001

Nishimoto, Y., Akiyama, Y., Shibasaki, R., 2016. Future Estimation Of Convenience Living Facilities Withdrawal Due To Population Decline All Over Japan From 2010 To 2040 - Focus On Supermarkets, Convenience Stores And Drugstores. Int. Arch. Photogramm. Remote Sens. Spatial Inf. Sci. XLI-B2, 223–226. https://doi.org/10.5194/isprs-archives-XLI-B2-223-2016

Open Government Data of Thailand, 2021. Bangkok Statistics (Social) Population Category.

Pajares, E., Muñoz Nieto, R., Meng, L., Wulfhorst, G., 2021. Population Disaggregation on the Building Level Based on Outdated Census Data. IJGI 10, 662. https://doi.org/10.3390/ijgi10100662

Rogers, D.J., Suk, J.E., Semenza, J.C., 2014. Using global maps to predict the risk of dengue in Europe. Acta Tropica 129, 1–14. https://doi.org/10.1016/j.actatropica.2013.08.008

Schug, F., Frantz, D., Linden, S. van der, Hostert, P., 2021. Gridded population mapping for Germany based on building density, height and type from Earth Observation data using census disaggregation and bottom-up estimates. PLOS ONE 16, e0249044. https://doi.org/10.1371/journal.pone.0249044

Shang, S., Du, Shihong, Du, Shouji, Zhu, S., 2021. Estimating building-scale population using multi-source spatial data. Cities 111, 103002. https://doi.org/10.1016/j.cities.2020.103002

Shepard, D., 1968. A two-dimensional interpolation function for irregularly-spaced data, in: Proceedings of the 1968 23rd ACM National Conference On -. Presented at the the 1968 23rd ACM national conference, ACM Press, Not Known, pp. 517–524. https://doi.org/10.1145/800186.810616

Smith, A., Bates, P.D., Wing, O., Sampson, C., Quinn, N., Neal, J., 2019. New estimates of flood exposure in developing countries using high-resolution population data. Nat Commun 10, 1814. https://doi.org/10.1038/s41467-019-09282-y

Sorichetta, A., Hornby, G.M., Stevens, F.R., Gaughan, A.E., Linard, C., Tatem, A.J., 2015. High-resolution gridded population datasets for Latin America and the Caribbean in 2010, 2015, and 2020. Sci Data 2, 150045. https://doi.org/10.1038/sdata.2015.45

Statistics Division, Bureau of General Affairs, 2022. TOKYO STATISTICAL YEARBOOK.

United Nations, Department of Economic and Social Affairs, Population Division, 2019. World Population Prospects 2019: Methodology of the United Nations population estimates and projections.

Vosselman, G., 2000. SLOPE BASED FILTERING OF LASER ALTIMETRY DATA.

Wang, S., Li, R., Jiang, J., Meng, Y., 2021. Fine-Scale Population Estimation Based on Building Classifications: A Case Study in Wuhan. Future Internet 13, 251. https://doi.org/10.3390/fi13100251

Weiss, D.J., Nelson, A., Vargas-Ruiz, C.A., Gligorić, K., Bavadekar, S., Gabrilovich, E., Bertozzi-Villa, A., Rozier, J., Gibson, H.S., Shekel, T., Kamath, C., Lieber, A., Schulman, K., Shao, Y., Qarkaxhija, V., Nandi, A.K., Keddie, S.H., Rumisha, S., Amratia, P., Arambepola, R., Chestnutt, E.G., Millar, J.J., Symons, T.L., Cameron, E., Battle, K.E., Bhatt, S., Gething, P.W., 2020. Global maps of travel time to healthcare facilities. Nat Med 26, 1835–1838. https://doi.org/10.1038/s41591-020-1059-1

Worldpop, 2013. Thailand 100m Population. https://doi.org/10.5258/SOTON/WP00267

Yang, C., Zhao, S., 2022. A building height dataset across China in 2017 estimated by the spatially-informed approach. Sci Data 9, 76. https://doi.org/10.1038/s41597-022-01192-x

Yao, Y., Liu, X., Li, X., Zhang, J., Liang, Z., Mai, K., Zhang, Y., 2017. Mapping fine-scale population distributions at the building level by integrating multisource geospatial big data. International Journal of Geographical Information Science 1–25. https://doi.org/10.1080/13658816.2017.1290252

Zandbergen, P.A., Ignizio, D.A., 2010. Comparison of Dasymetric Mapping Techniques for Small-Area Population Estimates. Cartography and Geographic Information Science 37, 199–214. https://doi.org/10.1559/152304010792194985

Zeng, C., Zhou, Y., Wang, S., Yan, F., Zhao, Q., 2011. Population spatialization in China based on night-time imagery and land use data. International Journal of Remote Sensing 32, 9599–9620. https://doi.org/10.1080/01431161.2011.569581